Supporting Information

Supporting Information

List of Figures

Supporting Information

List of Tables

Supporting Information

Literature screening process

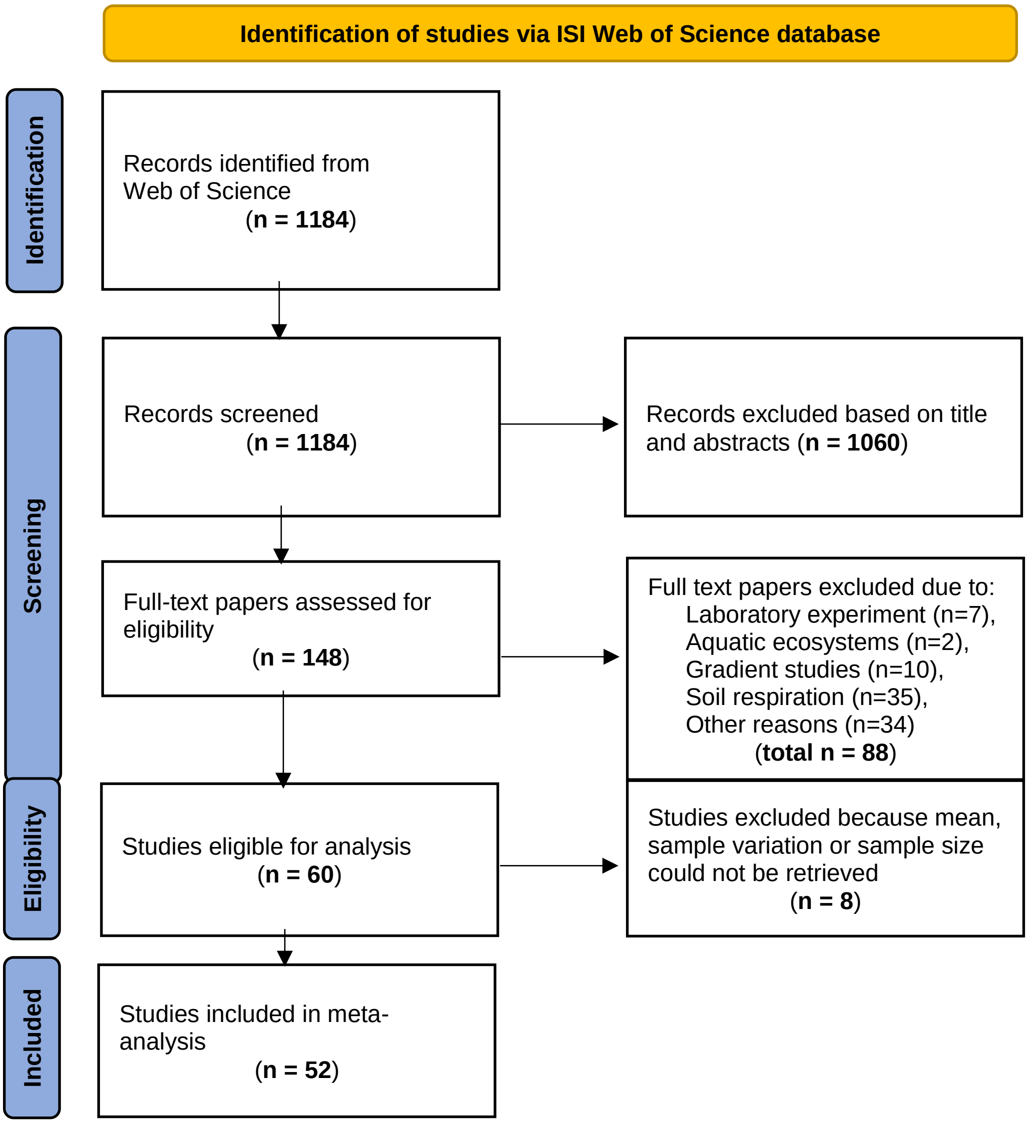

Figure S1 The literature screening process visualized as a preferred reporting items for systematic reviews and meta-analyses (PRISMA) flow diagram describing the number of screened studies (n) and exclusion rules in this meta-analysis.

Supporting Information

Peer-reviewed literature included in the meta-analysis

Table S1 Scientific research articles included in the meta-analysis, sorted by first author. The country of the study and used warming method (detailed information on the methods can be found in the original articles) of the reported study. Number of effect sizes per study (k), and sum of observations from ambient vs warmed treatments per study for the paired warming treatment and control.

Nr	Study	DOI	Country	Warming method	Effect sizes (*k*)	Obser-vations
1	Aerts et al., 2012	10.1007/s00442-012-2330-z	USA	Open-top chamber	6	30
2	Bélanger et al., 2023	10.3390/soilsystems7010014	Kazakhstan	Heating cable	24	480
3	Berbeco et al., 2012	10.1007/s11104-012-1130-x	USA	Heating cable	16	144
4	Berdugo et al., 2021	10.1007/s10021-020-00599-0	Spain	Open-top chamber	12	57
5	Bhuiyan et al., 2023	10.1016/j.scitotenv.2022.159683	Finland	Open-top chamber	50	300
6	Blok et al., 2016	10.1007/s10021-015-9924-3	Greenland	Open-top chamber	6	36
7	Blok et al., 2018	10.1111/gcb.14017	Greenland	Open-top chamber	4	20
8	Bokhorst et al., 2010	10.1016/j.soilbio.2009.12.011	Sweden	Infrared heater	12	72
9	Brigham et al., 2018	10.1080/15230430.2018.1494941	Belgium	Open-top chamber	4	16
10	Carbognani et al., 2014	10.1007/s11104-013-1982-8	Italy	Open-top chamber	4	20
11	Chen et al., 2008	10.2134/jeq2007.0266	USA	Sunlit controlled-environment chamber	2	78
12	Cheng et al., 2010	10.1016/j.agee.2010.04.019	Sweden	Infrared heater	14	70
13	Christiansen et al., 2017	10.1111/gcb.13362	Greenland	Open-top chamber	2	24
14	Chuckran et al., 2020	10.1016/j.soilbio.2020.107799	USA	Infrared heater	6	120
15	Cui et al., 2021	10.1007/s13157-021-01445-2	China	Open-top chamber	20	60
16	De Long et al., 2016	10.1016/j.soilbio.2016.04.009	Sweden	Open-top chamber	6	60
17	Gewirtzman et al., 2019	10.3389/fpls.2019.01097	USA	Heating cable	23	77
18	Gong et al., 2015	10.1371/journal.pone.0116013	China	Infrared heater	6	36
19	Han et al., 2019	10.3906/tar-1807-162	South Korea	Infrared heater	3	9
20	Henry et al., 2015	10.1007/s11104-014-2346-8	Canada	Infrared heater	8	80
21	Hong et al., 2021	10.1016/j.scitotenv.2020.142306	China	Open-top chamber	20	60
22	Kasurinen et al., 2017	10.1007/s11104-016-3122-8	Finland	Infrared heater	2	28
23	Li et al., 2022a	10.1016/j.soilbio.2022.108716	China	Heating cable	14	140

24	Li et al., 2022b	10.1093/jpe/rtac009	China	Infrared heater	1	8
25	Liu et al., 2021	10.1007/s11104-020-04551-y	China	Infrared heater	6	30
26	Liu et al., 2022	10.1016/j.geoderma.2022.116139	China	Heating cable	8	160
27	Lukas et al., 2018	10.1016/j.apsoil.2017.10.018	Germany	Heating cable	4	16
28	Luo et al., 2010	10.1111/j.1365-2486.2009.02026.x	China	Infrared heater	2	8
29	Luo et al., 2023	10.1098/rspb.2023.0613	China	Open-top chamber	8	160
30	McHale et al., 1998	10.1139/cjfr-28-9-1365	USA	Heating cable	12	108
31	Moise et al., 2014	10.1007/s00442-014-3068-6	Canada	Infrared heater	4	40
32	Morrison et al., 2019	10.1016/j.soilbio.2019.02.005	USA	Heating cable	1	10
33	Prieto et al., 2019	10.1111/1365-2745.13168	Spain	Open-top chamber	2	20
34	Remy et al., 2018	10.1007/s10021-017-0182-4	Netherlands	Open-top chamber	24	48
35	Ren et al., 2018	10.15302/J-FASE-2017194	China	Infrared heater	5	30
36	Robinson et al., 1995	10.2307/3545996	Sweden; Norway:Svalbard	Open-topped polythene tents	5	30
37	Robinson et al., 1997	10.1046/j.1365-2486.1997.d01-133.x	Sweden; Norway:Svalbard	Open-topped polythene tents	11	72
38	Romero-Olivares et al., 2017	10.1371/journal.pone.0179674	USA:Alaska	Open-top chamber	4	20
39	Rustad et al., 1998	10.2136/sssaj1998.03615995006200040031x	USA	Heating cable	6	40
40	Shaw et al., 2001	10.2307/3061022	USA	Infrared heater	34	176
41	Shu et al., 2019	10.1038/s41598-019-53450-5	China	Open-top chamber	2	8
42	Sjögersten et al., 2004	10.1023/B:PLSO.0000037044.63113.fe	Norway; Greenland	Open-top chamber	60	300
43	Sjögersten et al., 2012	10.1007/s10021-011-9514-y	Norway:Svalbard	Open-top chamber	4	20
44	Suseela et al., 2014	10.1016/j.soilbio.2014.03.022	USA	Infrared heater	6	36
45	Walter et al., 2013	10.1016/j.soilbio.2013.01.018	Germany	Infrared heater	1	15
46	Ward et al., 2015	10.1890/14-0292.1	UK	Open-top chamber	6	24
47	Xu et al., 2012	10.1111/j.1365-2389.2012.01449.x	China	Heating cable	9	36
48	Ye et al., 2022	10.1016\j.soilbio.2022.108588	China	Open-top chamber	12	576
49	Yin et al., 2022	10.1007/s00374-022-01639-8	China	Heating cable	4	32
50	Yoshitake et al., 2021	10.1111/grs.12319	Japan:Honshu	Infrared heater	8	48
51	Zaller et al., 2009	10.1111/j.1365-2486.2009.01970.x	Argentina:Tierra del Fuego	UVB filter film	8	40
52	Zhou et al., 2022	10.1093/jpe/rtac027	China	Infrared heater	2	16

Supporting Information

1. Aerts R, Callaghan TV, Dorrepaal E, Van Logtestijn RSP, Cornelissen JHC. 2012. Seasonal climate manipulations have only minor effects on litter decomposition rates and N dynamics but strong effects on litter P dynamics of sub-arctic bog species. *Oecologia* 170: 809–819.
2. Bélanger N, Chaput-Richard C. 2023. Experimental warming of typically acidic and nutrient-poor boreal soils does not affect leaf-litter decomposition of temperate deciduous tree species. *SOIL SYSTEMS* 7.
3. Berbeco MR, Melillo JM, Orians CM. 2012. Soil warming accelerates decomposition of fine woody debris. *Plant and Soil* 356: 405–417.
4. Berdugo M, Mendoza-Aguilar DO, Rey A, *et al.* 2021. Litter Decomposition Rates of Biocrust-Forming Lichens Are Similar to Those of Vascular Plants and Are Affected by Warming. *Ecosystems* 24: 1531–1544.
5. Bhuiyan R, Makiranta P, Strakova P, *et al.* 2023. Fine-root biomass production and its contribution to organic matter accumulation in sedge fens under changing climate. *SCIENCE OF THE TOTAL ENVIRONMENT* 858.
6. Blok D, Elberling B, Michelsen A. 2016. Initial Stages of Tundra Shrub Litter Decomposition May Be Accelerated by Deeper Winter Snow But Slowed Down by Spring Warming. *Ecosystems* 19: 155–169.
7. Blok D, Faucherre S, Banyasz I, Rinnan R, Michelsen A, Elberling B. 2018. Contrasting above- and belowground organic matter decomposition and carbon and nitrogen dynamics in response to warming in High Arctic tundra. *Global Change Biology* 24: 2660–2672.
8. Bokhorst S, Bjerke JW, Melillo J, Callaghan TV, Phoenix GK. 2010. Impacts of extreme winter warming events on litter decomposition in a sub-Arctic heathland. *Soil Biology and Biochemistry* 42: 611–617.
9. Brigham LM, Esch EH, Kopp CW, Cleland EE. 2018. Warming and shrub encroachment decrease decomposition in arid alpine and subalpine ecosystems. *Arctic, Antarctic, and Alpine Research* 50: e1494941.
10. Carbognani M, Petraglia A, Tomaselli M. 2014. Warming effects and plant trait control on the early-decomposition in alpine snowbeds. *Plant and Soil* 376: 277–290.
11. Chen H, Rygiewicz PT, Johnson MG, Harmon ME, Tian H, Tang JW. 2008. Chemistry and Long-Term Decomposition of Roots of Douglas-Fir Grown under Elevated Atmospheric Carbon Dioxide and Warming Conditions. *Journal of Environmental Quality* 37: 1327–1336.
12. Cheng X, Luo Y, Su B, *et al.* 2010. Experimental warming and clipping altered litter carbon and nitrogen dynamics in a tallgrass prairie. *Agriculture, Ecosystems & Environment* 138: 206–213.
13. Christiansen CT, Haugwitz MS, Priemé A, *et al.* 2017. Enhanced summer warming reduces fungal decomposer diversity and litter mass loss more strongly in dry than in wet tundra. *Global Change Biology* 23: 406–420.
14. Chuckran PF, Reibold R, Throop HL, Reed SC. 2020. Multiple mechanisms determine the effect of warming on plant litter decomposition in a dryland. *Soil Biology and Biochemistry* 145: 107799.
15. Cui W, Mao Y, Tian K, Wang H. 2021. A Comparative Study of Manipulative and Natural Temperature Increases in Controlling Wetland Plant Litter Decomposition. *Wetlands* 41: 48.
16. De Long JR, Dorrepaal E, Kardol P, Nilsson M-C, Teuber LM, Wardle DA. 2016. Understory plant functional groups and litter species identity are stronger drivers of litter decomposition than warming along a boreal forest post-fire successional gradient. *Soil Biology and Biochemistry* 98: 159–170.
17. Gewirtzman J, Tang J, Melillo JM, *et al.* 2019. Soil Warming Accelerates Biogeochemical Silica Cycling in a Temperate Forest. *Frontiers in Plant Science* 10: 1097.
18. Gong S, Guo R, Zhang T, Guo J. 2015. Warming and Nitrogen Addition Increase Litter Decomposition in a Temperate Meadow Ecosystem (M Schädler, Ed.). *PLOS ONE* 10: e0116013.
19. Han SH, Kim S, Chang H, Li G. 2019. Increased soil temperature stimulates changes in carbon, nitrogen, and mass loss in the fine roots of Pinus koraiensis under experimental warming and drought. *TURKISH JOURNAL OF AGRICULTURE AND FORESTRY* 43: 80–87.
20. Henry HAL, Moise ERD. 2015. Grass litter responses to warming and N addition: temporal variation in the contributions of litter quality and environmental effects to decomposition. *Plant and Soil* 389: 35–43.

21. Hong J, Lu X, Ma X, Wang X. 2021. Five-year study on the effects of warming and plant litter quality on litter decomposition rate in a Tibetan alpine grassland. *Science of The Total Environment* 750: 142306.
22. Kasurinen A, Silfver T, Rousi M, Mikola J. 2017. Warming and ozone exposure effects on silver birch (Betula pendula Roth) leaf litter quality, microbial growth and decomposition. *Plant and Soil* 414: 127–142.
23. Li A, Fan Y, Chen S, Song H, Lin C, Yang Y. 2022. Soil warming did not enhance leaf litter decomposition in two subtropical forests. *SOIL BIOLOGY & BIOCHEMISTRY* 170.
24. Li B, Lv W, Sun J, *et al.* 2022. Warming and grazing enhance litter decomposition and nutrient release independent of litter quality in an alpine meadow. *JOURNAL OF PLANT ECOLOGY* 15: 977–990.
25. Liu X, Chen S, Li X, *et al.* 2022. Soil warming delays leaf litter decomposition but exerts no effect on litter nutrient release in a subtropical natural forest over 450 days. *GEODERMA* 427.
26. Liu H, Lin L, Wang H, *et al.* 2021. Simulating warmer and drier climate increases root production but decreases root decomposition in an alpine grassland on the Tibetan plateau. *Plant and Soil* 458: 59–73.
27. Lukas S, Abbas SJ, Kössler P, Karlovsky P, Potthoff M, Joergensen RG. 2018. Fungal plant pathogens on inoculated maize leaves in a simulated soil warming experiment. *Applied Soil Ecology* 124: 75–82.
28. Luo B, Huang M, Wang W, *et al.* 2023. Ant nests increase litter decomposition to mitigate the negative effect of warming in an alpine grassland ecosystem. *PROCEEDINGS OF THE ROYAL SOCIETY B-BIOLOGICAL SCIENCES* 290.
29. Luo C, Xu G, Chao Z, *et al.* 2010. Effect of warming and grazing on litter mass loss and temperature sensitivity of litter and dung mass loss on the Tibetan plateau. *Global Change Biology* 16: 1606–1617.
30. McHale PJ, Mitchell MJ, Bowles FP. 1998. Soil warming in a northern hardwood forest: trace gas fluxes and leaf litter decomposition. *Canadian Journal of Forest Research* 28: 1365–1372.
31. Moise ERD, Henry HAL. 2014. Interactive responses of grass litter decomposition to warming, nitrogen addition and detritivore access in a temperate old field. *Oecologia* 176: 1151–1160.
32. Morrison EW, Pringle A, Van Diepen LTA, Grandy AS, Melillo JM, Frey SD. 2019. Warming alters fungal communities and litter chemistry with implications for soil carbon stocks. *Soil Biology and Biochemistry* 132: 120–130.
33. Prieto I, Almagro M, Bastida F, Querejeta JI. 2019. Altered leaf litter quality exacerbates the negative impact of climate change on decomposition (P Kardol, Ed.). *Journal of Ecology* 107: 2364–2382.
34. Remy E, Wuyts K, Van Nevel L, De Smedt P, Boeckx P, Verheyen K. 2018. Driving Factors Behind Litter Decomposition and Nutrient Release at Temperate Forest Edges. *Ecosystems* 21: 755–771.
35. Ren H, Qin J, Yan B, Alata, Baoyinhexige, Han G. 2018. Mass loss and nutrient dynamics during litter decomposition in response to warming and nitrogen addition in a desert steppe. *Frontiers of Agricultural Science and Engineering* 5: 64.
36. Robinson CH, Michelsen A, Lee JA, *et al.* 1997. Elevated atmospheric CO_2 affects decomposition of *Festuca vivipara* (L.) Sm. litter and roots in experiments simulating environmental change in two contrasting arctic ecosystems. *Global Change Biology* 3: 37–49.
37. Robinson CH, Wookey PA, Parsons AN, *et al.* 1995. Responses of Plant Litter Decomposition and Nitrogen Mineralisation to Simulated Environmental Change in a High Arctic Polar Semi-Desert and a Subarctic Dwarf Shrub Heath. *Oikos* 74: 503.
38. Romero-Olivares AL, Allison SD, Treseder KK. 2017. Decomposition of recalcitrant carbon under experimental warming in boreal forest (D Hui, Ed.). *PLOS ONE* 12: e0179674.
39. Rustad LE, Fernandez IJ. 1998. Soil Warming: Consequences for Foliar Litter Decay in a Spruce-Fir Forest in Maine, USA. *Soil Science Society of America Journal* 62: 1072–1080.
40. Shaw MR, Harte J. 2001. Control of Litter Decomposition in a Subalpine Meadow-Sagebrush Steppe Ecotone under Climate Change. *Ecological Applications* 11: 1206.
41. Shu M, Zhao Q, Li Z, Zhang L, Wang P, Hu S. 2019. Effects of global change factors and living roots on root litter decomposition in a Qinghai-Tibet alpine meadow. *Scientific Reports* 9: 16924.

42. Sjögersten S, Van Der Wal R, Woodin SJ. 2012. Impacts of Grazing and Climate Warming on C Pools and Decomposition Rates in Arctic Environments. *Ecosystems* 15: 349–362.
43. Sjögersten S, Wookey PA. 2004. Decomposition of mountain birch leaf litter at the forest-tundra ecotone in the Fennoscandian mountains in relation to climate and soil conditions. *Plant and Soil* 262: 215–227.
44. Suseela V, Tharayil N, Xing B, Dukes JS. 2014. Warming alters potential enzyme activity but precipitation regulates chemical transformations in grass litter exposed to simulated climatic changes. *Soil Biology and Biochemistry* 75: 102–112.
45. Walter J, Hein R, Beierkuhnlein C, *et al.* 2013. Combined effects of multifactor climate change and land-use on decomposition in temperate grassland. *Soil Biology and Biochemistry* 60: 10–18.
46. Ward SE, Orwin KH, Ostle NJ, *et al.* 2015. Vegetation exerts a greater control on litter decomposition than climate warming in peatlands. *Ecology* 96: 113–123.
47. Xu ZF, Pu XZ, Yin HJ, Zhao CZ, Liu Q, Wu FZ. 2012. Warming effects on the early decomposition of three litter types, Eastern Tibetan Plateau, China. *European Journal of Soil Science* 63: 360–367.
48. Ye C, Wang Y, Yan X, Guo H. 2022. Predominant role of air warming in regulating litter decomposition in a Tibetan alpine meadow: A multi-factor global change experiment. *SOIL BIOLOGY & BIOCHEMISTRY* 167.
49. Yin R, Qin W, Zhao H, Wang X, Cao G, Zhu B. 2022. Climate warming in an alpine meadow: differential responses of soil faunal vs. microbial effects on litter decomposition. *BIOLOGY AND FERTILITY OF SOILS* 58: 509–514.
50. Yoshitake S, Suminokura N, Ohtsuka T, Koizumi H. 2021. Composite effects of temperature increase and snow cover change on litter decomposition and microbial community in cool-temperate grassland. *Grassland Science* 67: 315–327.
51. Zaller JG, Caldwell MM, Flint SD, Ballaré CL, Scopel AL, Sala OE. 2009. Solar UVB and warming affect decomposition and earthworms in a fen ecosystem in Tierra del Fuego, Argentina. *Global Change Biology* 15: 2493–2502.
52. Zhou Y, Lv W-W, Wang S-P, *et al.* 2022. Additive effects of warming and grazing on fine-root decomposition and loss of nutrients in an alpine meadow. *JOURNAL OF PLANT ECOLOGY* 15: 1273–1284

Supporting Information

Locations of open-top chamber warming experiments measuring standardised plant litter (tea) decomposition

Table S2 Study sites in which standardised litter decomposition was measured in open-top chamber experiments. Observations per study are treatment replications in space and resulted in one effect size per site.

Nr	Site_ID	Site name	Country	Observations
1	ATA_1	Anchorage Island	Greenland	5
2	AUS_1	Australia	Australia	4
3	CAN_1	Common garden	Canada	12
4	CAN_2	Drained peatland	Canada	6
5	CAN_3	Kluane Elevation Transect 1	Canada	4
6	CAN_4	Kluane Elevation Transect 10	Canada	4
7	CAN_5	Kluane Elevation Transect 4	Canada	4
8	CAN_6	Kluane Elevation Transect 7	Canada	3
9	CAN_7	Plot B_dry	Canada	4
10	CAN_9	Pristine peatland	Canada	6
11	CHN_1	China meadow	China	18
12	CHN_2	China mountain	China	19
13	CHN_3	China swamp	China	18
14	CHN_4	National Field Observation and Research Station of Agro-ecosystems	China	9
15	ESP_1	Santa Olla	Spain	6
16	GRL_1	High_altitude - mesic mixed shrub tundra	Greenland	6
17	GRL_2	Low_altitude - mesic mixed shrub tundra	Greenland	6
18	ISL_1	Audkuluheidi	Iceland	20
19	ISL_2	Thingvellir	Iceland	19
20	ITA_1	Moss-snowbed	Italy	5
21	ITA_2	Shrub-snowbed	Italy	5
22	ITA_3	Po Valley	Italy	5
23	ITA_4	Northern Apennine	Italy	5
24	JPN_1	NKM2601	Japan:Honshu	10
25	JPN_2	Sapporo	Japan:Hokkaido	8
26	JPN_3	SGDG	Japan:Honshu	8
27	NOR_1	ITEX site Finse	Norway	17
28	NOR_2	Gudmedalen - low elevation	Norway	7
29	NOR_3	Kongsvoll Lower dry tundra	Norway	5
30	NOR_4	Kongsvoll Lower mesic tundra	Norway	4
31	NOR_5	Kongsvoll Upper mesic tundra	Norway	5
32	RUS_1	OTC experimental site, Eriophorum-Sphagnum bog	Russia	8
33	RUS_2	OTC experimental site, Sphagnum bog	Russia	8
34	SAU_1	Saudi Arabia	Saudi Arabia	10
35	SJM_1	Endalen - Cassiope heath	Norway:Svalbard	19
36	SJM_2	Endalen - Dryas heath	Norway:Svalbard	18
37	SJM_3	Endalen - Moss tundra	Norway:Svalbard	19
38	SJM_4	Endalen - Snowbed community	Norway:Svalbard	10
39	SJM_5	Svalbard_mesic	Norway:Svalbard	12

40	SJM_6	Svalbard_moist	Norway:Svalbard	14
41	SJM_7	Svalbard_wet	Norway:Svalbard	14
42	SWE_1	Abisko	Sweden	5
43	SWE_2	Latnajaure – Mesic meadow	Sweden	9
44	SWE_3	Latnajaure – Dry heath	Sweden	3
45	SWE_4	Latnajaure – Dry meadow	Sweden	5
46	SWE_5	Latnajaure – Wet meadow	Sweden	4
47	SWE_6	Latnajaure – Tussock tundra	Sweden	5
48	SWE_7	Latnajaure – Wet meadow	Sweden	5
49	USA_1	Atqasuk ITEX Dry Site	USA:Alaska	6
50	USA_2	Atqasuk ITEX Wet Site	USA:Alaska	6
51	USA_3	Barrow ITEX Dry Site	USA:Alaska	6
52	USA_4	Barrow ITEX Wet Site	USA:Alaska	6
53	ZAF_1	Cathedral Peak - grassland052rburn	South Africa	4
54	ZAF_2	Cathedral Peak - grassland0annual	South Africa	4
55	ZAF_3	Cathedral Peak - grassland0biennual	South Africa	4
56	ZAF_4	Cathedral Peak - grassland0noburn	South Africa	3
57	ZAF_5	Cathedral Peak - grassland0slope	South Africa	4

Supporting Information

Detailed Methodological Information

M1 - Calculation of Hedges' g

Hedges' g was calculated as calculated by dividing the difference between the mean mass loss in the warming treatment ($\bar{x}_1$) and ambient ($\bar{x}_2$) by the pooled standard deviation:

$$\text{Hedges' g} = \frac{(\bar{x}_1 - \bar{x}_2)}{\sqrt{((n_1 - 1) * s_1^2 \; + \; (n_2 - 1) * s_2^2) \; / \; (n_1 + n_2 - 2)}}$$

Eq. 3

where n_1 and n2 are sample size, and s12 and s22 are the sample variance of the warming treatment and ambient conditions, respectively.

M2 - Handling of Macro-Environmental Factors

To test the impact of macro-environment on the warming effect on decomposition, we first used multivariate linear mixed effects models (n=48) to explore whether the macro-environmental factors individually had a significant effect on the decomposition SMD (Table S6). However, as most environmental factors were confounded, we combined the macro-environmental factors to the underlying gradients using a Principal Component Analysis (PCA) on the scaled environmental variables using the R package FACTOMINER (v.2.4). We then used the four 'macro-environmental classes' created based on the origin of the PC1 and PC2 variables as a separation line, as moderator in the following multivariate linear mixed effects models to test whether the four environmental classes differed in their warming effect on decomposition. We used this factor 'class' as interacting moderator in the model to test for interactions in the macro-environment and the natural and standardised plant litter dataset.

M3 - Warming Methods and Micro-Environmental Effects

To test differences in the warming effect between the different warming methods used in the different studies and experiments (Table S1, 2), we used 'warming method' as moderator in another multivariate linear mixed effects model. In this model, the macro-environmental class was not integrated because the warming methods were not evenly distributed across the four macro-environmental classes (e.g., more OTC studies in higher latitudes). To test for differences in the warming methods in their effect on micro-environment, we used linear mixed-effects models (R package LMERTEST, v. 3.1-3) to test the overall effect of the categorical independent variable 'warming method' on the continuous dependent variables 'degree of warming' and 'warming-induced changes in soil moisture', respectively. We used Tukey HSD post-hoc tests (R packages MULTCOMP, v. 1.4-19 and EMMEANS, v. 1.7.5) to check for significant differences between the warming methods in degree of warming and warming-induced changes in soil moisture, respectively. We further tested with a linear regression for correlations between warming-induced changes in soil moisture and the degree of warming.

In addition, we tested the site-specific drivers related to environmental conditions (absolute latitude and, altitude), experimental setup (duration of warming before the experiment, mesh size) as individual moderators fitting separate multivariate linear mixed-effects models (Table S5).

Supporting Information

Macro-environmental factors

Table S3 Correlation off the map-based macro-environmental climatic factors to the Principal component axes (PC1, PC2) together with the units and sources, including WorldClim2 = database of high spatial resolution global weather and climate data, SoilGrids = system for global digital soil mapping, CGIAR=Consortium of International Agricultural Research Centers, EarthEnv = Global, remote-sensing supported environmental layers for assessing status and trends in biodiversity, ecosystems, and climate, MODIS=Moderate Resolution Imaging Spectroradiometer.

Variables	**Correlation coefficients**		**Unit**	**Global climate layer**	**Source**
	PCA1	**PCA2**			
Temperature					
Annual Mean Temperature	0.89	0.25	°C	WorldClim2	
Max Temperature of Warmest Month	0.86	0.09	°C	WorldClim2	
Air temperature isothermality	0.64	-0.19	unitless	WorldClim2	
Mean Diurnal Range	0.56	-0.35	°C	WorldClim2	
Mean Temperature of Coldest Quarter	0.81	0.28	°C	WorldClim2	
Mean Temperature of Driest Quarter	0.56	0.12	°C	WorldClim2	
Mean Temperature of Warmest Quarter	0.81	0.21	°C	WorldClim2	
Mean Temperature of Wettest Quarter	0.57	0.15	°C	WorldClim2	
Min Temperature of Coldest Month	0.68	0.33	°C	WorldClim2	
Annual Temperature Range	0.08	-0.26	°C	WorldClim2	
Temperature Seasonality	-0.19	-0.15	°C	WorldClim2	
Mean Temperature During Incubation Period	0.61	0.27	°C	WorldClim2	
Precipitation					
Annual Precipitation	0.46	0.77	mm	WorldClim2	
Precipitation of Coldest Quarter	0.20	0.82	mm	WorldClim2	
Precipitation of Driest Month	0.19	0.87	mm	WorldClim2	
Precipitation of Driest Quarter	0.24	0.88	mm	WorldClim2	
Precipitation of Warmest Quarter	0.40	0.39	mm	WorldClim2	
Precipitation of Wettest Month	0.51	0.41	mm	WorldClim2	

Precipitation of Wettest Quarter	0.51	0.46	mm	WorldClim2	
Precipitation Seasonality	0.13	-0.63	unitless	WorldClim2	
Sum Precipitation During Incubation Period	-0.01	0.32	mm	WorldClim2	
Soil					
Bulk density at 5 cm depth	0.73	-0.21	cg cm-3	SoilGrids	https://www.soilgrids.org
SOC Content at 5 cm depth	-0.78	0.29	dg kg-1	SoilGrids	https://www.soilgrids.org
SOC Density at 5 cm depth	-0.73	0.33	dg kg-1	SoilGrids	https://www.soilgrids.org
SOC Stock 0-5 cm depth	-0.49	0.57	kg m²	SoilGrids	https://www.soilgrids.org
Sum of Total Nitrogen at 5 cm depth	-0.53	0.62	cg kg-1	SoilGrids 2.0	https://www.soilgrids.org
Sum of Total Nitrogen at 15 cm depth	-0.76	0.21	cg kg-1	SoilGrids 2.0	https://www.soilgrids.org
Sum of Total Nitrogen at 30 cm depth	-0.76	0.08	cg kg-1	SoilGrids 2.0	https://www.soilgrids.org
Other					
Annal Mean Solar Radiation	0.77	-0.35	kJ/(m² day)	WorldClim2	
Aridity Index	-0.23	0.77	AI Value	CGIAR	http://www.cgiar-csi.org/data/global-aridity-and-pet-database
Aspect Cosine	0.06	-0.15	degree	TopoMed	https://www.earthenv.org/topography
Aspect Sine	-0.07	0.34	degree	TopoMed	https://www.earthenv.org/topography
Cover Barren	-0.53	-0.19	% (0-100)	Concensus	https://www.earthenv.org/landcover
Cover Cultivated	0.48	-0.31	% (0-100)	Concensus	https://www.earthenv.org/landcover
Cover Deciduous Broadleaf Trees	0.09	0.56	% (0-100)	Concensus	https://www.earthenv.org/landcover
Cover Evergreen Broadleaf Trees	0.14	0.22	% (0-100)	Concensus	https://www.earthenv.org/landcover
Cover Evergreen Needleleaf Trees	-0.02	0.16	% (0-100)	Concensus	https://www.earthenv.org/landcover
Cover Herbaceous	0.01	-0.54	% (0-100)	Concensus	https://www.earthenv.org/landcover
Cover Regularly Flooded	-0.17	0.03	% (0-100)	Concensus	https://www.earthenv.org/landcover
Cover Shrubs	-0.20	-0.06	% (0-100)	Concensus	https://www.earthenv.org/landcover
Eastness	-0.09	0.11	index (-1 to 1)	TopoMed	https://www.earthenv.org/topography
Elevation	0.15	-0.56	meters	TopoMed	https://www.earthenv.org/topography
Fraction Photosynthetically Active Radiation (fPAR)	0.54	0.65	Fpar fraction	MODIS	https://explorer.earthengine.google.com/#detail/MODIS%2F006%2FMCD15A3H
Soil water capacity at 5 cm depth	-0.56	0.05	%	SoilGrids	https://www.soilgrids.org

Supporting Information

Northness	0.28	-0.14	index (-1 to 1)	TopoMed	https://www.earthenv.org/topography
Potential Evapotranspiration (PET)	0.88	-0.29	PET Value (mm)	CGIAR	http://www.cgiar-csi.org/data/global-aridity-and-pet-database
Saturated Water Content 5 cm depth	-0.74	0.16	%	SoilGrids	https://www.soilgrids.org
Soil pH (water) at 5 cm depth	0.34	-0.78	pH x 10	SoilGrids	https://www.soilgrids.org

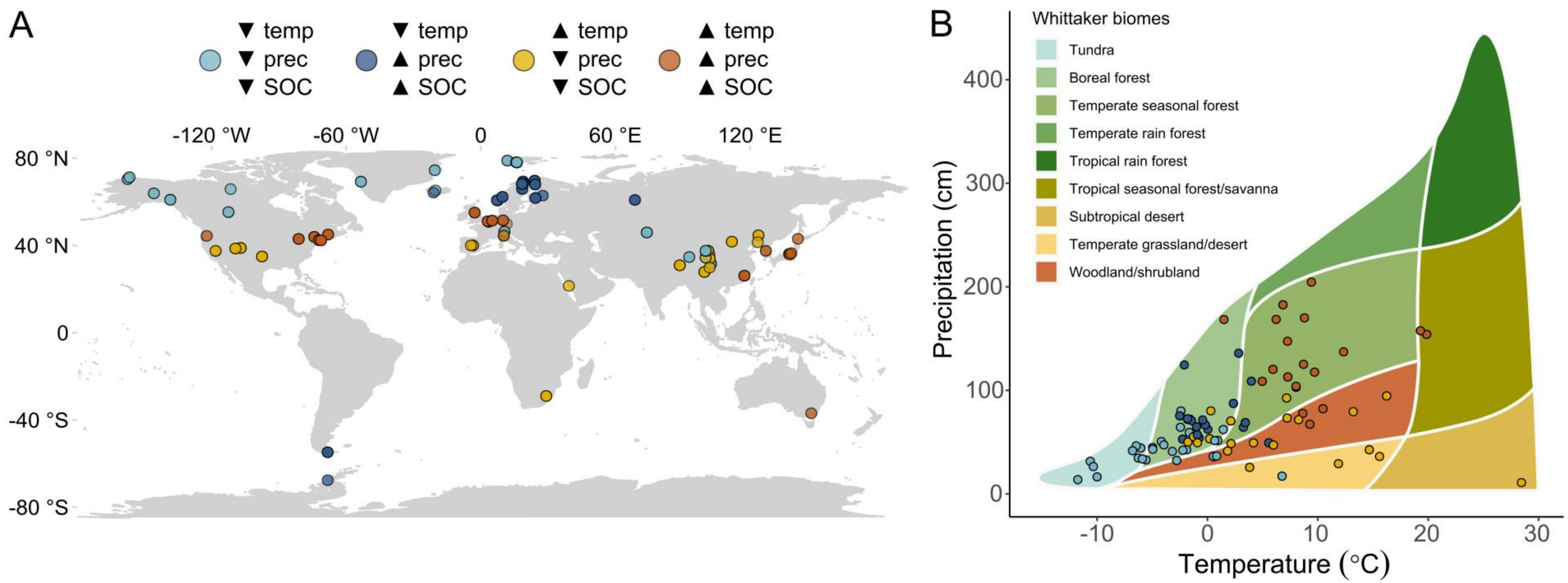

Figure S2 (**A**) Global distribution of study sites coloured according to the four main macro-environmental classes derived from the principal component analysis. (**B**) Study sites plotted in a Whittaker Biome Diagram with dots for study sites coloured according to the four main macro-environmental classes.

Supporting Information

Table S4 Means and standard error (SE) of the map-based macro-environmental factors per macro-environmental class that are defined by the scores on the PCA axis and the correlation of these axis to climatic variables of temperature (temp), precipitation (prec),Table S4 Means and standard error (SE) of the map-based macro-environmental factors per macro-environmental class that are defined by the scores on the PCA axis and the correlation of these axis to climatic variables of temperature (temp), precipitation (prec), and soil organic carbon (SOC) that are either high (upward arrow) or low (downward arrow).

Variables	Unit	▲ temp ▲ prec ▼ SOC			▲ temp ▼ prec ▼ SOC			▼ temp ▲ prec ▲ SOC			▼ temp ▼ prec ▲ SOC		
		mean		SE	mean		SE	mean		SE	mean		SE
Temperature													
Annual Mean Temperature	°C	9.3	±	0.3	5.6	±	0.5	0.3	±	0.2	-2.2	±	0.4
Max Temperature of Warmest Month	°C	24.6	±	0.3	22.8	±	0.5	15.5	±	0.2	14.7	±	0.5
Isothermality	unitless	31.1	±	0.3	37.8	±	0.4	25.4	±	0.3	23.7	±	0.5
Mean Diurnal Range	°C	9.8	±	0.1	12.9	±	0.1	7.4	±	0.1	8.0	±	0.2
Mean Temperature of Coldest Quarter	°C	-0.9	±	0.5	-4.4	±	0.6	-9.1	±	0.3	-13.5	±	0.4
Mean Temperature of Driest Quarter	°C	3.0	±	0.7	1.0	±	0.8	-3.9	±	0.4	-4.4	±	1.0
Mean Temperature of Warmest Quarter	°C	19.2	±	0.3	15.2	±	0.5	10.8	±	0.2	9.5	±	0.5
Mean Temperature of Wettest Quarter	°C	13.2	±	0.5	12.5	±	0.4	8.0	±	0.4	3.7	±	0.6
Min Temperature of Coldest Month	°C	-7.5	±	0.6	-12.2	±	0.6	-14.2	±	0.3	-19.1	±	0.4
Annual Temperature Range	°C	32.1	±	0.5	35.0	±	0.5	29.7	±	0.5	33.8	±	0.6
Temperature Seasonality	°C	819.1	±	15.0	799.5	±	17.5	807.1	±	15.0	945.5	±	19.8
Mean Temperature during Incubation Period	°C	11.1	±	0.5	6.7	±	0.6	1.4	±	0.4	2.4	±	0.5
Precipitation													
Annual Precipitation	mm	1172.4	±	24.4	554.2	±	15.3	642.1	±	13.7	357.5	±	13.1
Precipitation of Coldest Quarter	mm	241.6	±	7.1	67.1	±	4.2	141.6	±	5.5	58.5	±	2.7
Precipitation of Driest Month	mm	61.0	±	1.3	13.4	±	1.0	31.5	±	0.7	11.0	±	0.7
Precipitation of Driest Quarter	mm	204.4	±	3.7	49.9	±	3.2	103.4	±	2.2	42.6	±	2.2
Precipitation of Warmest Quarter	mm	337.4	±	12.4	224.4	±	8.6	208.9	±	2.6	140.9	±	7.2

Precipitation of Wettest Month	mm	142.5 ± 5.8	95.7 ± 2.9	85.1 ± 1.4	57.0 ± 2.6
Precipitation of Wettest Quarter	mm	399.8 ± 15.7	250.3 ± 7.4	228.1 ± 3.9	148.1 ± 6.9
Precipitation Seasonality	unitless	23.9 ± 1.7	63.5 ± 2.7	32.9 ± 0.6	47.4 ± 2.2
Sum Precipitation during Incubation Period	mm	820069.8 ± 56210.0	490908.5 ± 34505.2	912969.4 ± 47987.0	367516.6 ± 35516.5
Soil					
Bulk density at 5 cm depth	cg cm^{-3}	905.0 ± 17.6	1070.4 ± 20.9	504.9 ± 12.4	736.7 ± 11.1
SOC Content at 5 cm depth	dg kg^{-1}	78.9 ± 3.8	48.1 ± 2.1	142.8 ± 4.3	132.3 ± 3.8
SOC Density at 5 cm depth	dg kg^{-1}	620.9 ± 19.3	447.4 ± 15.4	783.2 ± 8.8	748.9 ± 10.3
SOC Stock 0-5 cm depth	kg m^2	41.2 ± 1.3	25.2 ± 0.8	38.1 ± 0.5	42.7 ± 0.7
Sum of Total Nitrogen at 5 cm depth	cg kg^{-1}	8776.1 ± 321.6	4561.7 ± 175.2	9632.6 ± 103.5	7817.3 ± 200.2
Sum of Total Nitrogen at 15 cm depth	cg kg^{-1}	3023.5 ± 78.2	2220.4 ± 61.1	5676.7 ± 163.6	5483.2 ± 191.8
Sum of Total Nitrogen at 30 cm depth	cg kg^{-1}	2007.3 ± 44.4	1639.6 ± 39.6	3506.9 ± 112.3	4508.9 ± 165.8
Other					
Annual Mean Solar Radiation	kJ/(m^2 day)	12532.0 ± 124.6	15999.4 ± 107.2	8170.1 ± 44.4	10200.2 ± 272.5
Aridity Index	AI Value	12066.2 ± 305.5	4484.7 ± 137.5	12164.9 ± 285.0	6978.2 ± 310.7
Aspect Cosine	degree	0.1 ± 0.0	0.0 ± 0.1	0.0 ± 0.1	0.3 ± 0.1
Aspect Sine	degree	0.2 ± 0.0	-0.2 ± 0.0	-0.1 ± 0.0	-0.1 ± 0.0
Cover Barren	% (0-100)	1.8 ± 0.4	5.3 ± 1.0	12.7 ± 1.3	26.2 ± 1.9
Cover Cultivated	% (0-100)	12.1 ± 1.5	26.1 ± 2.1	0.2 ± 0.1	3.7 ± 0.9
Cover Deciduous Broadleaf Trees	% (0-100)	23.8 ± 2.1	1.5 ± 0.2	5.9 ± 0.9	1.4 ± 0.3
Cover Evergreen Broadleaf Trees	% (0-100)	2.3 ± 0.5	0.0 ± 0.0	1.9 ± 0.7	0.0 ± 0.0
Cover Evergreen Needleleaf Trees	% (0-100)	6.5 ± 1.0	12.0 ± 1.8	17.2 ± 2.0	2.0 ± 0.3
Cover Herbaceous	% (0-100)	4.0 ± 1.4	40.8 ± 2.0	8.3 ± 0.9	24.1 ± 2.3
Cover Regularly Flooded	% (0-100)	0.0 ± 0.0	0.0 ± 0.0	4.1 ± 1.3	0.5 ± 0.2
Cover Shrubs	% (0-100)	0.1 ± 0.1	6.1 ± 1.1	19.7 ± 1.1	5.2 ± 1.2
Eastness	index (-1 to 1)	0.0 ± 0.0	0.0 ± 0.0	0.1 ± 0.0	0.0 ± 0.0
Elevation	meters	348.8 ± 31.2	2585.0 ± 111.3	436.8 ± 30.9	1034.8 ± 114.5
Fraction Photosynthetically Active Radiation (fPAR)	Fpar fraction	49.2 ± 0.8	28.4 ± 0.6	26.0 ± 0.5	17.6 ± 0.6

Supporting Information

Soil water capacity at 5 cm depth	%	22.6 ± 0.4	22.9 ± 0.3	27.0 ± 0.5	28.2 ± 0.2
Northness	index (-1 to 1)	0.1 ± 0.0	0.3 ± 0.0	0.0 ± 0.0	-0.1 ± 0.0
Potential Evapotranspiration (PET)	PET value (mm)	987.5 ± 14.0	1305.1 ± 22.5	534.4 ± 5.7	655.6 ± 27.5
Saturated Water Content 5 cm depth	%	57.2 ± 0.5	53.0 ± 0.6	69.2 ± 0.4	63.1 ± 0.3
Soil pH (water) at 5 cm depth	pH x 10	52.9 ± 0.5	68.3 ± 0.7	49.7 ± 0.3	61.0 ± 0.6

Supporting Information

Table S5 Results of single effects multivariate linear mixed-effects models for reported and measured site-specific environmental factors with the standardised mean difference of decomposition (SMD) as dependent and reported or measured site-specific environmental factors as predictor. Values in bold indicate significant effect of the predictor on decomposition SMD ($p \leq 0.05$). The number of effect sizes (*k*) used in the models, lower and upper bounds of the 95% confidence intervals, and heterogeneity explained by the model structure (Q_M) are reported.

Predictor	*k*	slope	95%CI	Test of Moderators (Qm, p-value)
Absolute Latitude	637	-0.002	-0.01, 0.01	0.25, p = 0.620
Duration of warming before experiment	637	0.06	-0.01, 0.12	3.23, p = 0.072
Mesh size	637	-0.045	-0.09, -0.003	**4.41, p = 0.036**
Carbon to Nitrogen ratio	428	0.001	-0.00, 0.00	0.94, p = 0.33
Ambient decomposability (mass loss % d^{-1})	613	-0.243	-0.45, -0.04	**5.60, p = 0.018**

Table S6 Map-based macro-environmental results of single multivariate linear mixed-effects models with the standardised mean difference of decomposition (SMD) as dependent variable and the map-derived macro-environmental factors as predictor. Values in bold indicate significant effect of the predictor on decomposition SMD ($p \leq 0.05$). The number of effect sizes (*k*) used in the models, lower and upper bounds of the 95% confidence intervals, and heterogeneity explained by the model structure (Q_M) are reported.

Predictor	*k*	slope	95%CI	Test of Moderators (Qm, p-value)
Temperature				
Annual Mean Temperature	635	0.010	-0.00, 0.02	2.07, p = 0.150
Max Temperature of Warmest Month	635	0.008	-0.01, 0.02	1.21, p = 0.270
Air temperature isothermality	635	0.001	-0.01, 0.01	0.02, p = 0.894
Mean Diurnal Range	635	-0.016	-0.05, 0.02	0.89, p = 0.375
Mean Temperature of Coldest Quarter	635	0.007	-0.00, 0.02	1.42, p = 0.233
Mean Temperature of Driest Quarter	635	0.003	-0.00, 0.01	0.68, p = 0.411
Mean Temperature of Warmest Quarter	635	0.012	-0.00, 0.03	2.37, p = 0.124
Mean Temperature of Wettest Quarter	635	0.006	- 0.01, 0.02	0.83, p = 0.361
Min Temperature of Coldest Month	635	0.008	-0.00, 0.02	1.88, p = 0.171
Annual Temperature Range	635	-0.003	-0.02, 0.01	0.22, p = 0.639
Temperature Seasonality	635	-0.000	-0.00, 0.00	0.00, p = 0.981
Mean Temperature during Incubation Period	625	-0.007	-0.02, -0.00	2.08, p = 0.149
Precipitation				
Annual Precipitation	635	0.000	-0.00, 0.00	0.00, p = 0.974
Precipitation of Coldest Quarter	635	0.000	-0.00, 0.00	1.13, p = 0.288
Precipitation of Driest Month	635	0.004	0.00, 0.01	**3.97, p = 0.046**
Precipitation of Driest Quarter	635	0.001	-0.00, 0.00	3.33, p = 0.068
Precipitation of Warmest Quarter	635	-0.000	-0.00, 0.00	0.36, p = 0.550

Precipitation of Wettest Month	635	0.000	-0.00, 0.00	0.00, p = 0.973
Precipitation of Wettest Quarter	635	-0.000	-0.00, 0.00	0.01, p = 0.906
Precipitation Seasonality	635	0.001	-0.00, 0.00	0.39, p = 0.535
Sum Precipitation during Incubation Period	625	0.000	-0.00, 0.00	1.27, p = 0.259
Soil				
Bulk density at 5 cm depth	635	0.000	-0.00, 0.00	0.04, p = 0.844
SOC Content at 5 cm depth	635	0.000	-0.02, 0.01	0.03, p = 0.855
SOC Density at 5 cm depth	635	0.000	-0.00, 0.00	0.20, p = 0.656
SOC Stock 0-5 cm depth	635	0.000	-0.01, 0.01	0.01, p = 0.904
Sum of Total Nitrogen at 5 cm depth	604	0.000	-0.00, 0.00	0.01, p = 0.904
Sum of Total Nitrogen at 15 cm depth	604	0.000	-0.00, 0.00	0.00, p = 0.997
Sum of Total Nitrogen at 30 cm depth	604	0.000	-0.00, 0.00	0.03, p = 0.861
Other				
Annal Mean Solar Radiation	635	0.000	-0.00, 0.00	0.36, p = 0.547
Aridity Index	635	0.000	-0.00, 0.00	0.30, p = 0.583
Aspect Cosine	635	-0.031	-0.13, 0.07	0.39, p = 0.532
Aspect Sine	635	-0.103	-0.25, 0.05	1.81, p = 0.179
Cover Barren	635	0.003	-0.01, 0.003	0.90, p = 0.342
Cover Cultivated	635	-0.002	-0.01, 0.003	0.49, p = 0.483
Cover Deciduous Broadleaf Trees	635	0.004	0.002, 0.01	1.49, p = 0.222
Cover Evergreen Broadleaf Trees	635	-0.009	-0.01, 0.03	0.78, p = 0.372
Cover Evergreen Needleleaf Trees	635	-0.002	-0.01, 0.00	0.23, p = 0.634
Cover Herbaceous	635	0.002	-0.00, 0.00	0.01, p = 0.912
Cover Regularly Flooded	635	0.004	-0.00, 0.01	1.14, p = 0.285
Cover Shrubs	635	0.000	-0.01, -0.01	0.02, p = 0.884
Eastness	635	-0.006	-0.35, 0.34	0.00, p = 0.974
Elevation	635	-0.000	-0.00, 0.00	1.96, p = 0.162
Fraction Photosynthetically Active Radiation (fPAR)	635	0.000	-0.01, 0.01	0.01, p = 0.911
Soil water capacity at 5 cm depth	635	-0.001	-0.02, 0.02	0.01, p = 0.923
Northness	635	-0.240	-0.44, -0.04	**5.44, p = 0.020**
Potential Evapotranspiration (PET)	635	0.000	-0.00, 0.00	1.97, p = 0.161
Saturated Water Content 5 cm depth	635	-0.002	-0.01, 0.01	0.12, p = 0.732
Soil pH (water) at 5 cm depth	635	-0.003	-0.01, 0.01	0.24, p = 0.625

Supporting Information

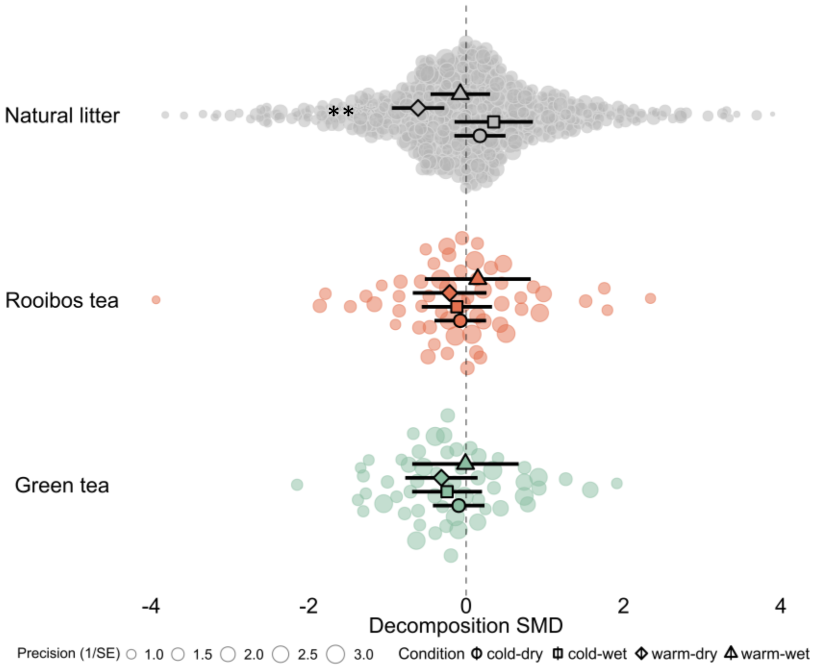

Figure S3 Effects of experimental warming on plant litter decomposition. The pooled average decomposition standardised mean difference (SMD, Hedges' g; outlined circles) and 95% confidence intervals (black error bars) resulting from warming for the macro-environmental classes cold and dry (outlined circles), cold and wet (outlined squares), warm and dry (outlined diamonds), and warm and wet (outlined triangles) for the natural litter (blue, number of effect sizes k=523) and the standardised plant litter, separated into rooibos (red, k=57) and green tea (green, k=57). Each coloured dot is an individual effect size (non-outlined circles) with dot size representing its precision (the inverse of the standard error, larger points having greater influence on the model). Asterisks indicate that the overall pooled average SMD is significantly different from zero (**p < 0.01).

Table S7 The impact of the four macro-environmental classes four macro-environmental classes distinguished by different combinations of high (▲) or low (▼) of temperature (temp), precipitation (prec) and soil organic carbon (SOC) and the natural and the standardised plant litter (i.e., green and rooibos tea) on the effect of warming on decomposition (SMD). Bold values indicate a significant effect of the macro-environmental class and litter type on SMD (p ≤ 0.05 or CI ≠ 0). Number of effect sizes (*k*), p-values, and 95%-confidence interval are shown.

Macro-environment	**litter type**	**SMD estimate**	***k***	**p-value**	**95%CI**
▲ temp ▲ prec ▼ SOC	Natural litter	-0.07	155	0.703	[-0.45; 0.30]
	Rooibos	-0.15	5	0.666	[-0.82; 0.52]
	Green	0.01	5	0.981	[-0.67; 0.68]
▲ temp ▼ prec ▼ SOC	Natural litter	**-0.61**	150	**<0.001**	[-0.94; -0.28]
	Rooibos	0.21	10	0.382	[-0.26; 0.68]
	Green	0.31	10	0.180	[-0.15; 0.77]
▼ temp ▲ prec ▲ SOC	Natural litter	0.35	126	0.167	[-0.15; 0.85]
	Rooibos	0.12	15	0.607	[-0.33; 0.56]
	Green	0.24	15	0.285	[-0.20; 0.69]
▼ temp ▼ prec ▲ SOC	Natural litter	0.18	101	0.290	[-0.15; 0.50]
	Rooibos	0.07	27	0.659	[-0.25; 0.40]
	Green	0.09	15	0.575	[-0.23; 0.42]

Supporting Information

The effect of experimental-induced warming on decomposition

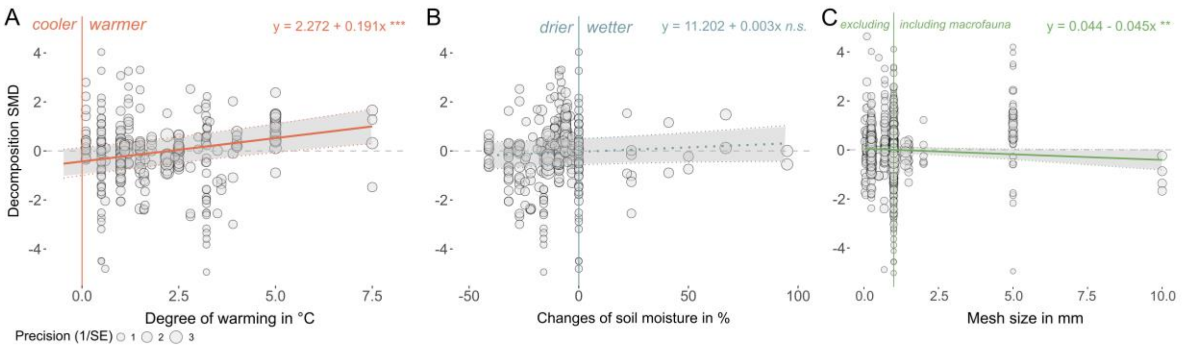

Figure S4 Impacts of experimentally induced changes in micro-environment on decomposition. Effect of **(A)** degree of warming (i.e., absolute temperature difference between warmed and control plots, k=315); **(B)** warming-induced changes in soil moisture with warming (i.e., difference between warmed and control plots in soil moisture, k=315) on decomposition SMD; and **(C)** mesh size of the litter bags in mm with 1 mm as the minimal threshold for macrofauna exclusion (Sagi and Hawlena 2024). Each grey outlined circle is an individual effect size with circle size representing its precision (the inverse of the standard error, larger points having greater influence on the model). Asterisks indicate that the overall pooled average SMD is significantly different from zero. Solid lines indicate regression lines with shaded areas representing the 95%CI (***p < 0.001, **p < 0.01). Dashed lines indicate no significant relationship (n.s. = not significant).

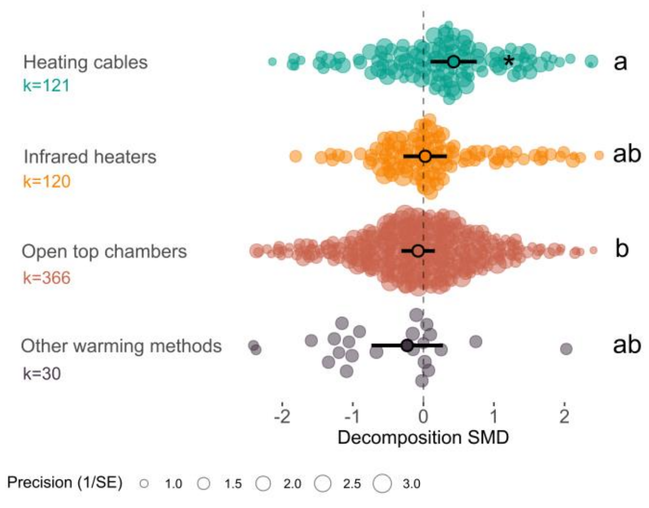

Figure S5 Impact of warming methods on decomposition SMD. The pooled average decomposition standardised mean difference (SMD, Hedges' g; outlined circles) and 95% confidence intervals (black error bars) resulting from warming for the different experimental warming methods (see Table S1). Each coloured dot is an individual effect size (non-outlined circles) with dot size representing its precision (the inverse of the standard error, larger points having greater influence on the model). Letters indicate significant differences between the pooled average SMD of warming methods. Asterisks indicate a significant deviation of decomposition SMD from zero (*p ≤ 0.05).

Supporting Information

Plant functional types and plant organ types interacting with the position of incubation (on soil surface, buried in the soil)

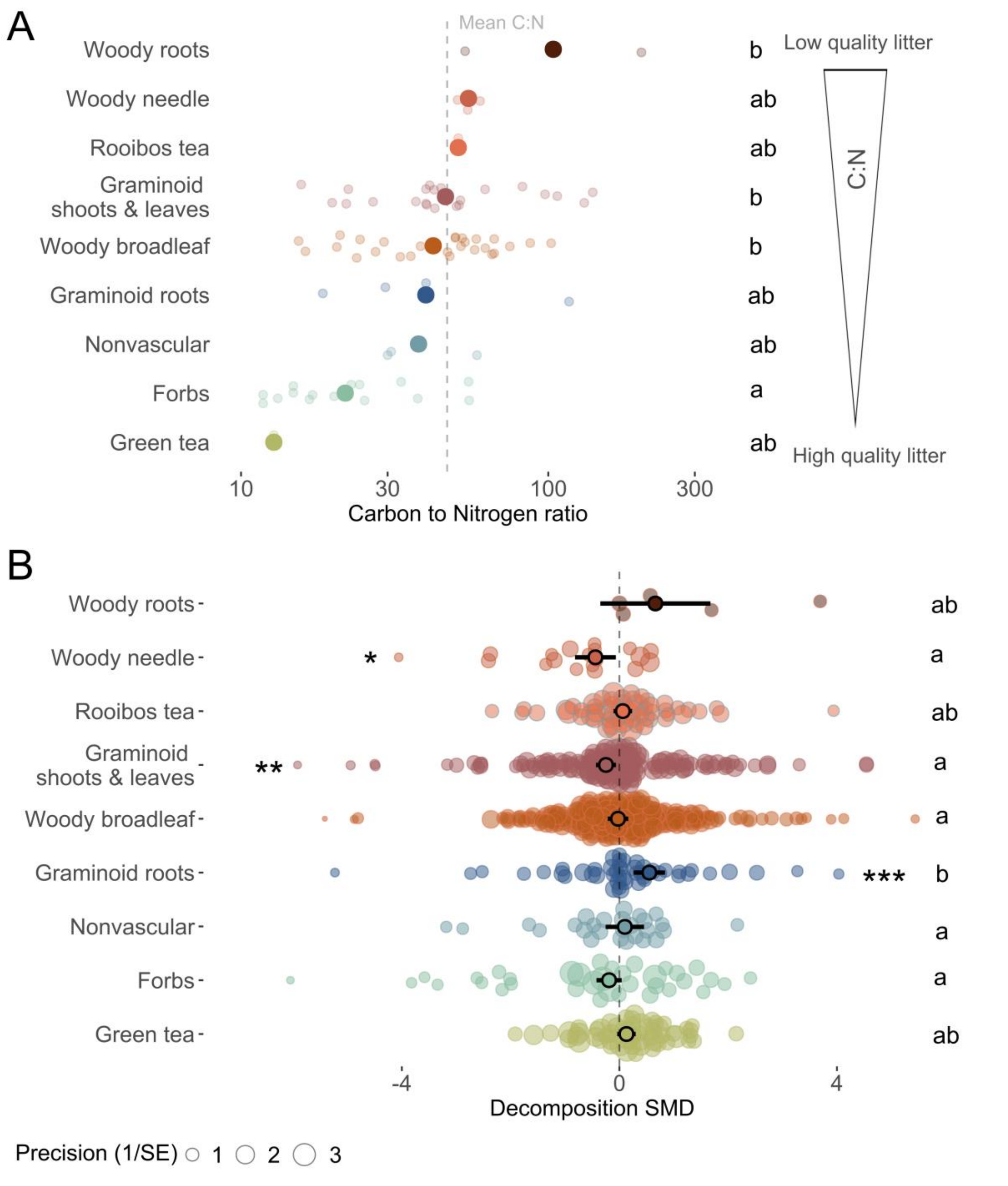

Figure S6 Differences in C:N ratio and warming effect on decomposition across plant functional types**. (A)** Plant functional types ranked based on carbon to nitrogen ratios (C:N ratios). Large, coloured points represent mean C:N ratios and small transparent dots individual plant species. **(B)** The pooled average decomposition standardized mean difference (SMD, Hedges' g, black outlined circles) and 95% confidence intervals (95%CI, black error bars) per plant functional type of natural litter and standardised plant litter combining data from above and below ground incubations. Different letters indicate differences in **(A)** mean C:N ratio and **(B)** decomposition SMD between the different plant functional litter types, as well as the standard material green and rooibos tea. Asterisks indicate that the overall pooled average SMD is significantly different from zero (*p < 0.05, **p < 0.01, ***p < 0.001).

Supporting Information

Table S8 The pooled average decomposition standardised mean difference (SMD) of different plant functional types of the natural litter and natural and the standardised plant litter (i.e., green and rooibos tea) with respect to the position of incubation (i.e., on soil surface, buried in the soil) as well as the number of effect sizes (*k*) for each category, the p-value and 95%-confidence interval describing whether the pooled average SMD significantly differs from zero (in bold, p ≤ 0.05). For forbs and nonvascular plants no reports of buried or root litter were available.

Plant functional type	Position incubated	*k*	SMD estimate	p-value	95%CI
Forb	surface	36	-0.19	0.114	[-0.42; 0.05]
Graminoid root	buried	49	**0.55**	**<0.001**	[0.27; 0.84]
Graminoid shoot/leaf	surface	151	**-0.25**	**0.010**	[-0.43; -0.06]
Green tea	buried	57	0.13	0.133	[-0.04; 0.30]
Nonvascular	surface	27	0.10	0.589	[-0.26; 0.45]
Rooibos tea	buried	57	0.06	0.469	[-0.11; 0.23]
Woody broadleaf	buried	48	-0.05	0.799	[-0.44; 0.34]
Woody broadleaf	surface	192	-0.02	0.874	[-0.21; 0.18]
Woody needle	surface	21	**-0.44**	**0.021**	[-0.82; -0.07]
Woody root	buried	5	0.35	0.337	[-0.37; 1.08]

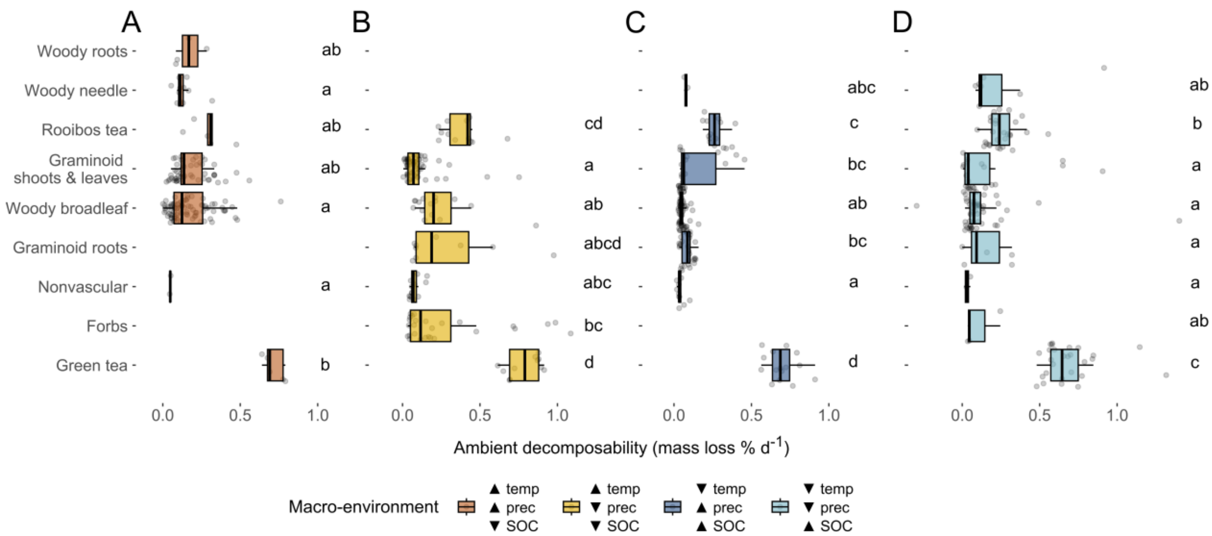

Figure S7 Differences in ambient decomposability, measured as ambient mass loss rate per day (% d^{-1}), for the plant functional types and plant organs of natural plant litter and the standardised tea material (i.e., rooibos and green tea) for each of the four macro-environmental classes. Colours indicate the four macro-environmental classes of temperature (temp), precipitation (prec) and soil organic carbon (SOC) that are either high (▲) or low (▼), consistent with Figure 3 in the main text. Different letters indicate significant differences in decomposition SMD between plant functional types.